

See discussions, stats, and author profiles for this publication at: <https://www.researchgate.net/publication/238562138>

Natural steric analysis: ab initio van der Waals radii of atoms and ions. J Chem Phys

ARTICLE *in* THE JOURNAL OF CHEMICAL PHYSICS · OCTOBER 1997

Impact Factor: 2.95 · DOI: 10.1063/1.475149

CITATIONS

94

READS

121

2 AUTHORS, INCLUDING:



Frank Weinhold

University of Wisconsin–Madison

199 PUBLICATIONS 28,503 CITATIONS

SEE PROFILE

Natural steric analysis: Ab initio van der Waals radii of atoms and ions

J. K. Badenhoop and F. Weinhold

Citation: *J. Chem. Phys.* **107**, 5422 (1997); doi: 10.1063/1.475149

View online: <http://dx.doi.org/10.1063/1.475149>

View Table of Contents: <http://jcp.aip.org/resource/1/JCPSA6/v107/i14>

Published by the [American Institute of Physics](#).

Additional information on J. Chem. Phys.

Journal Homepage: <http://jcp.aip.org/>

Journal Information: http://jcp.aip.org/about/about_the_journal

Top downloads: http://jcp.aip.org/features/most_downloaded

Information for Authors: <http://jcp.aip.org/authors>

ADVERTISEMENT



**ALL THE PHYSICS
OUTSIDE OF
YOUR JOURNALS.**

www.physicstoday.org
**physics
today**

Natural steric analysis: *Ab initio* van der Waals radii of atoms and ions

J. K. Badenhoop^{a)} and F. Weinhold

Theoretical Chemistry Institute and Department of Chemistry, University of Wisconsin, Madison, Wisconsin 53706

(Received 2 November 1995; accepted 1 July 1997)

We employ natural steric analysis (introduced in a previous paper) to evaluate a set of effective *ab initio* van der Waals radii for free and covalently bonded atoms and ions of H–Ar ($Z=1-18$) determined using a helium atom probe. We critically examine the degree of anisotropy, dependence on charge state, and other intrinsic limitations of a simple atomic van der Waals hard sphere representation of the accurate steric surface. We also evaluate the *ab initio* steric force (gradient of steric energy at van der Waals contact) as a measure of “hardness” of the atomic van der Waals spheres. Comparison with empirical van der Waals radii shows reasonable agreement (within the acknowledged uncertainties of the latter values in the most important cases), but suggest a wider range of variability and anisotropy than could be adequately represented by any fixed constant radius. Simple expressions for incorporating the dependence on natural atomic charge or correcting for other types of intermolecular contact are given, extending the accuracy and usefulness of the atomic van der Waals sphere concept. © 1997 American Institute of Physics.
[S0021-9606(97)00538-2]

I. INTRODUCTION

Steric repulsions and the associated “effective volumes” of nonbonded atoms or functional groups play a fundamental role in the theory of intra- and intermolecular interactions. The nonbonded radius or “van der Waals radius” has been often used as a measure of atomic size since Pauling proposed representative values for this purpose.¹ However, such radii can be measured or calculated by many different methods.² Classical empirical potential forms usually include an attractive force (e.g., of dispersion type) and a repulsive force associated with steric exchange interactions.³ Whereas the attractive term is of long range (e.g., R^{-6}) and dominates at longer distances, the repulsive force acts over a shorter range, usually taken to be an exponential (Born–Mayer) or R^{-n} (e.g., Lennard-Jones $n=12$) function of distance. These empirical forms have been incorporated into the force fields of commonly used molecular modeling programs (MM3,⁴ AMBER,⁵ CHARMM,⁶ MIP,⁷ UFF,⁸ etc.) Traditionally the van der Waals contact distance has been defined as the distance at which the van der Waals potential is a minimum and this distance as the sum of the two atomic radii; the functional form is scaled to this distance as a parameter. Pauling’s van der Waals radii were determined from average contact distances in molecular crystals, and refined by Bondi⁹ using improved x-ray diffraction data. Many refinements of Pauling’s approach have subsequently been considered.

Allinger³ has contended that the van der Waals distances used by Pauling and Bondi were actually “distances of closest approach” in the crystal environment, and the attractive dispersion forces from distant atoms bring the molecules closer than the sum of their van der Waals radii. In order to estimate the true pairwise van der Waals potential, he scaled

the potential function to make the attractive term for each like-atom interaction approximate that of the corresponding rare gas in the same row of the periodic table, while adjusting the other parameters to fit available thermochemical data. His set of van der Waals radii exceed Pauling’s values by 8%–20%.

The assumption of a spherical atomic radius was studied by Zefirov and Porai-Koshits,¹⁰ Row and Parnathy,¹¹ and Nyburg and Faerman¹² who correlated minimum van der Waals contact distance with contact angle for like atoms in a large number of molecular crystals. They found that the atomic radius in a molecular environment is better described as elliptical, with the major axis perpendicular to the bond and the minor axis along the bond, called “polar flattening.”

Bartell¹³ and Glidewell¹⁴ defined a set of nonbonded “one-angle” radii based on the distance of closest approach of atoms X and Y in a fragment XMY, which set a limit on the effective radius of each atom in the direction of the other in the molecular environment, usually well within van der Waals contact. These radii fall below Pauling’s values and were found to correlate well with Bondi’s van der Waals radii.¹⁵ However, this definition of the radius is internal to the three atom fragment rather than showing the exterior van der Waals surface of the fragment. Charton^{16,17} used a similar definition to calculate effective minimum and maximum van der Waals radii and volumes for a large number of functional groups.

The definition of an “ionic radius” has also been formulated by many different methods. Pauling¹⁸ postulated that the interatomic distances in ionic crystals were the equilibrium configuration resulting from the competition of Coulomb attraction between oppositely charged ions, the repulsive force from the overlap of the ion electron distributions, and if like-charged anions (generally larger than cations) are in contact, Coulomb “double repulsion.” He used these contact distances to derive a set of empirical “crystal radii” for

^{a)}Present address: Department of Math and Sciences, Potomac State College of West Virginia, Keyser, WV 26726.

ions with common valences, comparing them to previous values proposed by Goldschmidt.¹⁹ Gourary and Adrian²⁰ found that electron distribution maps calculated using improved x-ray crystallographic techniques showed that cations were up to 0.2 Å larger and anion 0.2 Å smaller than the additive radius approximation predicts. Narayan²¹ defined an ionic crystal radius using a repulsive “compression energy” between two ions, an exponentially decreasing function of distance opposed by an arbitrarily chosen constant attractive force reflecting the crystal environment in alkyl halides. From the fitted potential parameters he defined a univalent and multivalent radius and a “compressibility” (gradient of the force with respect to pressure) for a selection of ions. In line with the results of Gourary and Adrian, Narayan’s cation radii were larger and anions smaller than predicted by Pauling because of the lower compressibility of cations compared to anions. Pauling also recognized that ionic crystal radii are dependent on the coordination number of the ion and suggested a correction factor for liganacy.²² Thus empirical ionic radii determined by these methods are found to be strongly dependent on crystal environment.

In biological systems, ionic radii appropriate to (aqueous) solution are required. Marcus²³ calculated radii for ions in solution using the results of neutron and x-ray diffraction on liquid samples coupled with Monte Carlo and molecular dynamics simulations, obtaining values that agreed well with Pauling’s crystal radii. Shanker and Agrawal²⁴ also took account of polarizability-related variations of ionic radii, noting that the polarizabilities of ions in a crystal differ markedly from those of free ions.

The “size” of an ion is determined by the distribution of the outermost electrons, and Pauling defined an ionic radius in terms of an effective nuclear charge attracting these electrons. Sanderson²⁵ estimated ionic radii by noting the dependence of the average electronic density (electrons per unit volume) of an ion in a crystal on its electronegativity as defined by Pauling.²⁶ The dependence of the radius of an atom or ion on charge density and net charge was also recognized by Thomas,²⁷ who calculated the radius from an integrated form of the electron density distribution. Others have defined atomic or ionic radii as the distance at which the density reaches a certain universal value²⁸ or as the zero or minimum of a proposed electron density functional,²⁹ but the absolute radii show strong dependence on the form of the functional (and thus are not considered further). Stokes³⁰ found a charge-dependent decrease in ionic radii across iso-electronic series calculated from hydration energies. Miertus *et al.*³¹ correlated these variations with atomic charges calculated by Mulliken population analysis. They found the best fit to be a function of the form

$$r_i = \exp(a_i q_i + b_i), \quad (1)$$

where r_i is the radius of atom i , q_i is the net charge, and a_i , b_i are fitted parameters. For the purpose of eliminating energetically unfavorable conformations, Iijima and co-workers³² defined a radius based on steric exchange repulsion connected to the volume into which another atom or group cannot intrude without exceeding a certain repulsive interaction

energy.³³ They calibrated Pauling’s van der Waals radii such that molecular models assuming hard sphere radii reproduced the amino acid conformations in proteins and peptides observed by x-ray crystallography; the adjusted values were smaller than Pauling’s by 4%–10%.

In a previous paper³⁴ (designated Paper I) we presented a natural bond orbital³⁵ (NBO)-based method for calculating the overall repulsive exchange energy of a system as the sum of relative orbital energy changes of individual NBOs $\{\bar{\sigma}_I\}$ upon orthogonalization from their preorthogonalized counterparts (PNBOs) $\{\sigma_I\}$:

$$E_{\text{exchange}}^{\text{NBO}} = \sum_I E_I^x, \quad (2)$$

where

$$E_I^x = F_{I,I}^{\text{NBO}} - F_{I,I}^{\text{PNBO}} \quad (3)$$

and $F_{I,I}^{\text{NBO}} = \langle \bar{\sigma}_I | \hat{\mathcal{F}} | \bar{\sigma}_I \rangle$, $F_{I,I}^{\text{PNBO}} = \langle \sigma_I | \hat{\mathcal{F}} | \sigma_I \rangle$, $\hat{\mathcal{F}}$ being the Fock operator. The steric exchange repulsion energy between two atoms or molecules A and B is then

$$\Delta E_{\text{steric}}^{\text{NBO}} = E_{\text{exchange}}^{\text{NBO}}(A \cdots B) - [E_{\text{exchange}}^{\text{NBO}}(A) + E_{\text{exchange}}^{\text{NBO}}(B)]. \quad (4)$$

This method was applied to various atom–molecule interactions, and an NBO-based “van der Waals contact” distance was defined as the distance at which the steric repulsion energy becomes comparable to ambient thermal energy, kT

$$\Delta E_{\text{steric}}^{\text{NBO}}(R_{\text{vdw}}) = 298k = 0.592 \text{ kcal/mol}. \quad (5)$$

The steric van der Waals radii of the rare-gas atoms were shown to be approximately additive, and an *ab initio* van der Waals radius of a molecule in a certain direction was defined as the interaction distance between a molecule and a helium probe atom (along the angle of approach) at which Eq. (5) is true, less the rare-gas atom radius. (Helium was chosen because of its small size and low polarizability.) However, the steric van der Waals contact distance between two molecules was shown to depend on the full electronic distributions of both molecules, rather than only those of orbitals in direct contact, leading to nonadditivity of these radii, overestimated in some cases, underestimated in others. For complexes with strong intermolecular charge transfer (e.g., hydrogen bonding), the steric exchange energy and steric contact distance are also strongly dependent on the accompanying orbital polarization and shift of the charge distribution. Thus for the purpose of calculating effective van der Waals radii, we consider only contacts with weak intermolecular delocalization (<1.5 kcal/mol) or polarization (molecular dipole moment within 0.1 Debye of the isolated species), in which the steric exchange potential is monotonically repulsive. We will show that deviations from additivity are systematic for most of these contacts.

In this paper, we present a set of effective van der Waals radii (based on a helium probe) for free and bound atoms and ions from the first three rows of the periodic table. We describe an approximate calibration of these helium-based radii to other atomic and molecular probes, correcting the additive

TABLE I. Calculated steric van der Waals radii (in angstroms) of isolated atoms and common ions for the first three rows of the Periodic Table (6-31G* basis). Also given (in brackets) is the gradient of the steric potential $[d(\Delta E_{\text{steric}}^{\text{NBO}})/dr]_{r_l}$ (kcal/mol per Å), or the “steric force” exerted on the helium probe, at van der Waals contact.

Atomic radii							
H							He
1.781							1.069
[2.31]							[3.14]
Li	Be	B	C	N	O	F	Ne
2.843	2.216	1.776	1.619	1.432	1.358	1.209	1.216
[1.14]	[1.84]	[1.91]	[2.34]	[3.13]	[2.83]	[4.40]	[3.19]
Na	Mg	Al	Si	P	S	Cl	Ar
3.067	2.753	2.296	2.208	2.034	1.911	1.858	1.779
[1.03]	[1.36]	[1.31]	[1.66]	[1.93]	[2.08]	[2.38]	[2.59]
Ionic radii							
						H ⁻	He
						1.662	1.069
						[2.44]	[3.14]
Li ⁺	Be ²⁺			N ³⁻	O ²⁻	F ⁻	Ne
0.869	0.751			1.898	1.624	1.378	1.216
[3.90]	[5.64]			[2.66]	[2.88]	[3.01]	[3.19]
Na ⁺	Mg ²⁺			P ³⁻	S ²⁻	Cl ⁻	Ar
1.133	1.004			2.720	2.392	2.059	1.779
[3.32]	[5.25]			[2.09]	[2.13]	[2.36]	[2.59]

estimates to more accurately reflect the actual intermolecular steric van der Waals contact distances. All calculations were performed using the GAUSSIAN 92³⁶ electronic structure package. The paper is organized as follows: Section II presents van der Waals radii for free atoms and ions. Section III compares radii calculated from the “end-on” or “most exposed” approach of He to an atom in a molecule, and discusses the dependence on atomic charge. In Sec. IV we estimate the degree of anisotropy by calculating the steric surface at angles perpendicular to the most exposed direction, or toward molecular “crevices.” Section V discusses the basis set and probe dependence of steric van der Waals radii, presenting an approximate procedure to correct the helium-based effective radius of an atom for alternate molecular probes. Section VII presents a summary and concluding remarks.

II. VAN DER WAALS RADII OF FREE ATOMS AND IONS

The atomic radii for the elements through argon calculated at the HP/6-31G* level by the procedure described above are listed in the top half of Table I. Also given (in brackets) is the gradient of the steric potential or “steric force” exerted on the helium probe at van der Waals contact, $[d(\Delta E_{\text{steric}}^{\text{NBO}})/dr]_{r_l}$.

The calculated natural steric radii of Table I follow the expected periodic trends, despite alternating between closed- and open-shell treatments. Except for hydrogen, these radii also compare favorably with the van der Waals radii estimated by Pauling (H:1.2 Å, N:1.5 Å, O:1.40 Å, F:1.35 Å, P:1.9 Å, S:1.85 Å, Cl:1.80 Å).¹ Pauling’s hydrogen radius was estimated from intermolecular contacts which involved

hydrogen bonding, causing closer contact than van der Waals forces alone would predict, hence a smaller radius than our value.

Table I also lists radii for common ions with noble gas electron configurations. In general these radii are direct reflections of the exchange repulsion between the electron distribution of the ion and that of the helium probe, reasonably free of donor–acceptor interactions (<1.5 kcal/mol delocalization energy). However, radii for trivalent ions such as Al³⁺ cannot be obtained by this method, since there is strong donation from the He 1s orbital into the empty electrophilic *p* orbitals of the cation, artificially inflating the NBO exchange energy and exaggerating the radius. (More accurate radii should be obtained by using a *like cation* as a probe.) One expects that the radii should decrease over the isoelectronic series (H⁻ to Be²⁺, N³⁻ to Mg²⁺, P³⁻ to Ar), since the number of electrons in the filled orbitals is the same but the nuclear charge increases; this and other reasonable periodic trends are observed to hold. Note that the noble gases fit smoothly into both sets of radii. Each cation is proportionally smaller than its corresponding neutral atom, and each anion larger, as expected.

The “hardness” of the radius can be measured by the gradient of the potential (the amount of “steric force” necessary to push the probe and the probed species closer together) at the steric radius. The valence electrons of a neutral alkali or alkaline earth metal are more loosely held than the valence electrons of a nonmetal in the same row. From this argument one expects the electron distribution of the metal to be “softer” and thus more easily penetrated than the nonmetal. The gradient of the NBO exchange repulsion potential is consistent with this hypothesis; the steric force is lower for Li (1.14 kcal/Å mol) than for F (4.40). To put these values in perspective, one can express the force in terms of the increase of temperature beyond ambient temperature (298 K) needed to compress the helium probe atom 0.1 Å inside van der Waals contact. For the Li atom, this temperature increase is 57.37 K while for F it is 221.43 K. One can also see from the steric potential gradients that the cations are “harder” than anions, consistent with the empirical results of Narayan.²¹ In fact, the potential is quite steep for the approach to the more highly charged cations, reflecting a slow rise (or even decrease) in steric exchange energy as the neutral He approaches the ion and its electron distribution is attracted to the net positive charge. However, eventually the He orbitals overlap the denser core orbitals of the cation, causing a sudden rise in repulsion energy. In a sense this phenomenon is an artifact of using a helium probe in this method, yet distortion of the orbitals to enhance donor–acceptor interactions would occur even more strongly for interactions of cations with other species.

Notice that certain free ions (such as H⁻) are not bound at HF levels of theory. However, within the restrictions of the Hartree–Fock approximation and a finite basis set, NBO steric analysis can be used to define a theoretical steric radius of these species, even if purely as a point of comparison with atoms and ions in a molecular environment.

III. VAN DER WAALS RADII OF ATOMS IN MOLECULES

NBO steric analysis was also used to find the steric effective van der Waals radii of atoms in a representative selection of molecules (HF/6-31G* optimized geometry), tabulated in Table II. We first obtain a "longitudinal radius" (r_l) in the direction in which an atom is most exposed. For atoms in the terminal position, this is along the direction of a bond. For other atoms with more than one bond, it is the direction furthest from all bonded atoms. The longitudinal radii correspond most nearly to an atomic van der Waals radius.

We first notice that within this set of data, there is a clear difference between the radius of an atom in a covalent compound as compared to an ionic compound. Since Li_2 and F_2 are electroneutral and LiF is a strongly ionic salt with almost unit charges (± 0.924), we can compare their radii with the free atom or ion radii. The lithium radius in Li_2 (2.700 Å) and fluorine radius in F_2 (1.273 Å) are closer to the free atomic radii (Li:2.843 Å, F:1.209 Å), while those of LiF (Li:1.394 Å, F:1.431 Å) are close to the free ion radii (Li^+ :0.869 Å, F^- :1.378 Å). Atoms with intermediate net charge generally have radii that fall in between the free atom and ion values. The free atom and ion radii in Table I should *not* be confused with the more practical longitudinal values in Table II.

For a given atom, there is a correlation between the steric radius of an atom and its natural charge, i.e., the more positive the charge, the smaller the radius. Plots of natural charge versus steric van der Waals radius for H, F, and Cl are shown in Figs. 1–3. Also shown are the best linear fits of this data:

$$\begin{aligned} r_{\text{H}} &= 1.43 - 0.41q_{\text{H}}, \\ r_{\text{F}} &= 1.27 - 0.15q_{\text{F}}, \\ r_{\text{Cl}} &= 1.89 - 0.16q_{\text{Cl}}. \end{aligned} \quad (6)$$

Exponential forms analogous to those used by Miertus *et al.*³¹ gave significantly poorer fits.

In general, the steric radius increases as more net electron density is centered on that atom. Over the series CH_4 , NH_3 , H_2O , HF , the H–X bond polarizes more toward the heavy atom and away from hydrogen. Thus the hydrogen "envelope" contracts, yielding a lower steric energy and allowing the probe atom to penetrate closer given the same energy. However, a methyl or methylene hydrogen radius varies by only ± 0.01 Å for this limited set of examples, and steric radii should be transferable to the same degree as natural charge among different molecules. Fluorine and chlorine show the same dependence on net electron density or charge. One common characteristic is that the atomic radii in homonuclear diatomic molecules (H_2 , N_2 , O_2 , F_2 , P_2 , S_2 , Cl_2) are smaller than their neutral atomic charge would predict, relative to atomic radii in other molecules. This is consistent with the findings of Zefirov and Porai-Koshits¹⁰ that the nearest-neighbor van der Waals contact in solid Cl_2 (3.28 Å) falls in the lower end of the range of nearest-neighbor C–Cl \cdots Cl–C van der Waals contacts in molecular crystals

TABLE II. Longitudinal van der Waals radii r_l (Å), measured end-on along a bond, for a provisional selection of ionic and covalent molecules. Also listed is the gradient of the steric potential (kcal/mol per Å) at van der Waals contact.

Atom	Molecule	Natural charge	r_l	$[d(\Delta E_{\text{steric}}^{\text{NBO}})/dr]_{r_l}$
H	LiH	−0.725	1.645	2.13
	BH ₃	−0.128	1.461	2.31
	C ₂ H ₆	+0.212	1.426	2.39
	CH ₄	+0.216	1.420	2.46
	C ₂ H ₄	+0.206	1.415	2.24
	C ₂ H ₂	+0.239	1.396	2.31
	H ₂	0.000	1.394	2.27
	CH ₃ F	+0.171	1.391	2.36
	CH ₃ Cl	+0.233	1.377	2.35
	H ₂ CO	+0.123	1.374	2.31
	HCN	+0.232	1.372	2.23
	H ₂ S	+0.131	1.362	2.44
	CH ₃ SH	+0.110	1.360	2.45
	CH ₃ F ₂	+0.145	1.354	2.36
	H ₂ CS	+0.213	1.338	2.39
	CH ₂ Cl ₂	+0.252	1.329	2.44
	NH ₃	+0.370	1.329	2.30
	HNC	+0.461	1.321	2.33
	CHF ₃	+0.139	1.309	2.59
	HCl	+0.276	1.287	2.53
	CHCl ₃	+0.270	1.276	2.54
	CH ₃ OH	+0.476	1.247	2.49
	HNO	+0.290	1.222	2.58
	H ₂ O	+0.477	1.200	2.46
	HF	+0.520	1.103	2.61
He	He	0.000	1.069	2.14
Li	Li ₂	0.000	2.700	1.57
	LiH	+0.725	2.128	1.15
	LiF	+0.924	1.394	2.97
Be	Be ₄	0.000	2.613	1.82
	BeO	+1.592	0.921	14.11
B	B ₂ O	+0.645	2.255	2.22
	BN	+0.901	0.654	20.32
C	HNC	+0.461	1.924	2.54
	CO	+0.610	1.885	2.55
N	NH ₃	−1.111	1.834	2.74
	HNO	−0.001	1.756	2.75
	NF ₃	+0.807	1.748	3.08
	HCN	−0.349	1.739	2.59
	NP	−0.878	1.728	2.72
	AlN	−0.892	1.718	2.39
	N ₂	0.000	1.678	2.71
	NO	+0.285	1.529	2.75
O	MgO	−1.190	1.738	2.04
	Al ₂ O ₃	−1.283	1.688	2.21
	H ₂ O	−0.955	1.583	2.98
	CH ₃ OH	−0.791	1.582	3.07
	BeO	−1.592	1.578	2.22
	B ₂ O ₃	−0.896	1.538	2.72
	H ₂ CO	−0.578	1.532	2.69
	CO	−0.610	1.514	2.73
	OS	−0.685	1.507	2.94
	CO ₂	−0.622	1.506	3.13
	HNO	−0.289	1.493	2.75
	NO	−0.285	1.478	2.89
	OF ₂	+0.259	1.467	3.08
	O ₂	0.000	1.438	2.89

TABLE II. (Continued.)

Atom	Molecule	Natural charge	r_l	$[d(\Delta E_{\text{steric}}^{\text{NBO}})/dr]_{r_l}$
F	LiF	-0.924	1.431	3.18
	PF ₃	-0.639	1.357	2.01
	BF ₃	-0.556	1.354	2.99
	CH ₃ F	-0.429	1.348	3.37
	CH ₂ F ₂	-0.429	1.347	3.24
	C ₂ F ₄	-0.371	1.343	3.15
	CHF ₃	-0.421	1.342	3.13
	CF ₄	-0.405	1.334	3.01
	HF	-0.520	1.326	3.16
	NF ₃	-0.269	1.314	3.08
	OF ₂	-0.130	1.298	3.15
	F ₂	0.000	1.273	3.09
Ne	Ne	0.000	1.216	3.19
Na	Na ₂	0.000	3.156	1.14
	NaCl	+0.937	1.674	2.32
Mg	Mg ₄	0.000	2.742	1.39
	MgO	+1.190	2.225	1.57
Al	Al ₂ O	+0.830	2.914	1.48
	AlN	+0.892	1.049	16.92
P	PH ₃	+0.126	2.541	1.95
	P ₄	0.000	2.444	2.28
	PF ₃	+1.918	2.393	2.01
	P ₂	0.000	2.379	2.07
	NP	+0.878	2.340	2.03
S	CH ₃ SH	-0.030	2.226	2.19
	S ₈	0.000	2.222	2.43
	H ₂ S	-0.263	2.190	2.17
	CS ₂	+0.157	2.139	2.08
	H ₂ CS	+0.039	2.133	2.12
	S ₂	0.000	2.068	2.24
Cl	OS	+0.685	2.046	2.23
	NaCl	-0.937	2.046	2.46
	CH ₃ Cl	-0.100	1.943	2.36
	CH ₂ Cl ₂	-0.042	1.918	2.34
	HCl	-0.276	1.905	2.41
	CHCl ₃	+0.012	1.893	2.33
	CCl ₄	+0.059	1.871	2.44
Cl ₂		0.000	1.857	2.42
Ar	Ar	0.000	1.779	2.59

(3.25–3.65 Å). For the three monovalent elements cited above, the linear fit is comparatively good because they always occur as bond termini. The data for the other elements was either too limited or the atom's environment too variable to derive a useful relation based on net charge alone.

Although the atomic radius varies among different molecules, we can give recommended or representative values for each atomic radius, as shown in Table III. A superscript “F” indicates the best value is that of the free atom radius, while “M” indicates a value calculated from a fit to the data in Table II. Table III also displays the wide range of other values (up to ~0.6 Å for some elements) which have been proposed for the van der Waals radius. The recommended steric radii are plotted in Fig. 4 for the Group VA–VIIIA

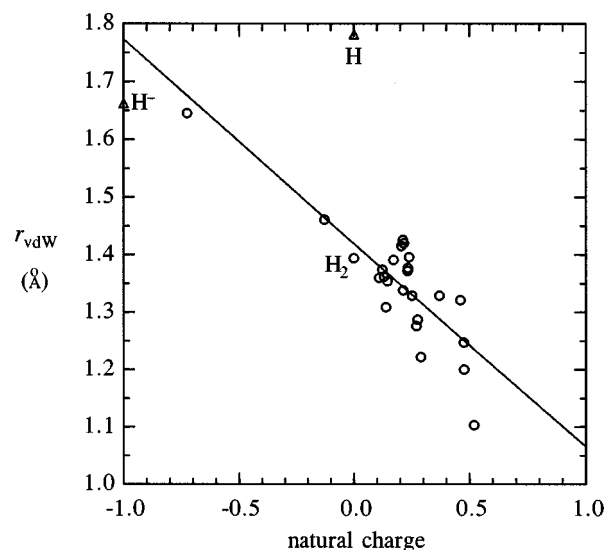


FIG. 1. Dependence of H steric radius on the natural charge. Shown are H radii in molecules (circles) and the free atom H and ion H⁻ (triangles). The radius of H₂ is also labeled.

elements, with Pauling's empirical values shown for comparison. Most of the recommended natural steric radii for second row atoms are within the range of covalent and ionic crystal radii Pauling averaged to estimate a van der Waals radius. The radii for third row elements are somewhat larger than Pauling's values, probably due to the fact that van der Waals and electrostatic interactions bring crystalline non-metal atoms inside the distance predicted by steric repulsion alone.

While there are observable variations in the natural steric radius of an atom depending on its molecular environment, from these recommended values one can see that the atomic

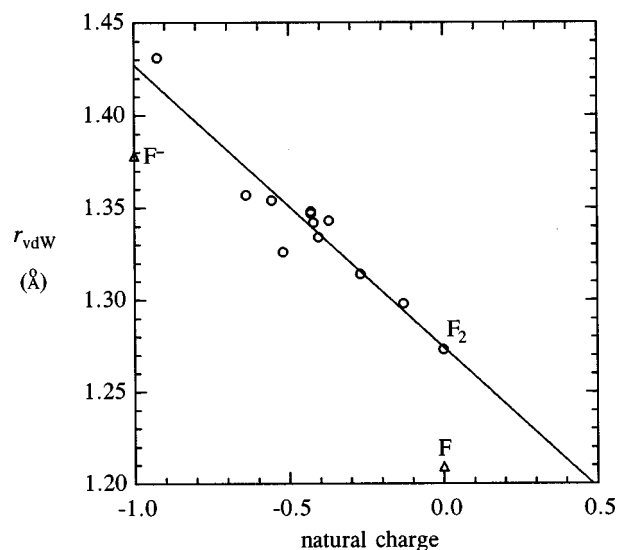


FIG. 2. Dependence of F steric radius on natural charge. Shown are F radii in molecules (circles) and the free atom F and ion F⁻ (triangles). The radius of F₂ is also labeled.

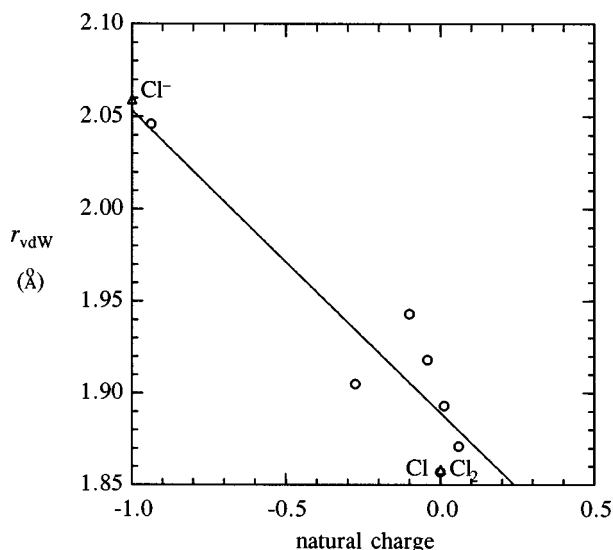


FIG. 3. Dependence of H steric radius on natural charge. Shown are Cl radii in molecules (circles) and the free atom Cl and ion Cl^- (triangles). The radius of Cl_2 is also labeled.

radii of covalent compounds follow the expected periodic trends, i.e., the radius decreases across each row Li–Ne and Na–Ar, and increases with atomic weight within a period. This can be seen most clearly in the series N_2 ($r_{\text{N}} = 1.678 \text{ Å}$), O_2 ($r_{\text{O}} = 1.438 \text{ Å}$), F_2 ($r_{\text{F}} = 1.273 \text{ Å}$), Ne (r_{Ne}

TABLE III. Recommended values for NBO steric van der Waals atomic radii, with comparison nonbonded radii estimated by previous methods. Pauling's values for rare-gas radii extrapolated from crystal radii. (Superscript "F" denotes free atom value, "M" denotes a representative intermediate value from entries in Table II).

Atom	$r_{\text{steric}}^{\text{NBO}}$	Previous values
H	1.42 ^M	1.20, ^a 1.20, ^d 1.50, ^g 1.16, ^e 1.08 ^h
He	1.07 ^F	(0.93), ^a 1.40, ^d 1.48 ^g
Li	2.76 ^M	1.82, ^d 2.10, ⁱ 1.55 ^b
Be	(2.22) ^F	1.12, ^b 1.39, ^f 1.80 ⁱ
B	(1.78) ^F	2.13, ^d 1.33, ^f 1.80, ^g 1.75, ⁱ 0.98 ^b
C	(1.62) ^F	1.70, ^a 1.70, ^d 1.71, ^e 1.25, ^f 1.85(sp, sp^2), ^g 1.75(sp^3), ^g 1.70 ⁱ
N	1.63 ^M	1.50, ^a 1.55, ^d 1.50, ^e 1.14, ^f 1.70, ^g 1.45, ^h 1.60 ⁱ
O	1.46 ^M	1.40, ^a 1.52, ^d 1.29, ^e 1.13, ^f 1.65, ^g 1.50 ⁱ
F	1.27 ^M	1.35, ^a 1.47, ^d 1.40, ^e 1.08, ^f 1.60, ^g 1.40 ⁱ
Ne	1.22 ^M	(1.12), ^a 1.60, ^b 1.58, ^c 1.54, ^d 1.54, ^g 1.50 ⁱ
Na	(3.07) ^F	1.86, ^b 2.27, ^d 2.30 ⁱ
Mg	(2.75) ^F	1.60, ^b 1.73, ^d 2.20 ⁱ
Al	(2.30) ^F	1.43, ^b 2.51, ^d 1.66, ^f 2.00 ⁱ
Si	(2.21) ^F	2.10, ^d 1.55, ^f 2.10, ^g 1.95 ⁱ
P	2.44 ^M	1.90, ^a 1.45, ^f 2.05, ^g 1.90 ⁱ
S	2.16 ^M	1.85, ^a 1.80, ^d 1.84, ^e 1.45, ^f 2.00, ^g 1.85 ⁱ
Cl	1.89 ^M	1.80, ^a 1.75, ^d 1.90, ^e 1.44, ^f 1.95, ^g 1.80 ⁱ
Ar	1.78 ^F	(1.54), ^a 1.92, ^b 1.88, ^d 1.90 ⁱ

^aReference 1, pp. 260, 514.

^bReference 25.

^cReference 30.

^dReference 9.

^eReferences 10 and 41.

^fReference 14.

^gReference 3, p. 17.

^hReference 32.

ⁱReference 2.

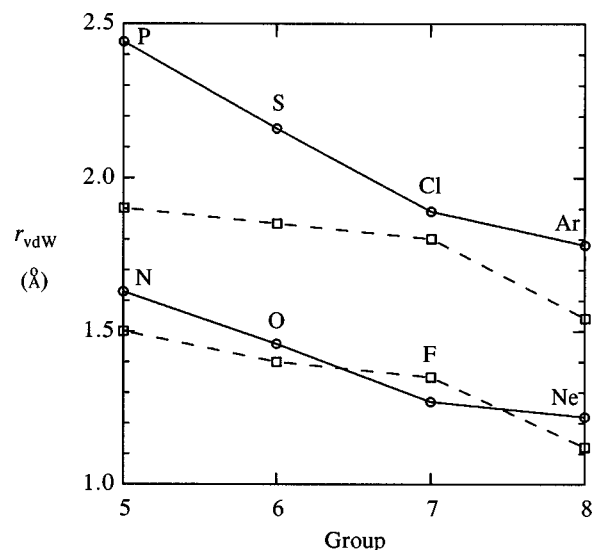


FIG. 4. Van der Waals radii for Group VA–VIII A elements of the second and third periods, as calculated from natural steric analysis (circles, solid lines). Empirical Pauling values (squares, dashed lines) are shown for comparison.

$= 1.216 \text{ Å}$). In contrast the covalent radius for the three diatomics (N_2 :0.539 Å, O_2 :0.584 Å, F_2 :0.673 Å) is increasing as the bond order decreases. In a sense this is counterintuitive, because one expects a more diffuse electron distribution as the number of lone pairs increases. However, this tendency is outweighed by the increasing positive nuclear charge, which decreases orbital radius.

The steric exchange potential gradients of covalent and ionic species are also listed in Table II. The longitudinal steric forces for atoms in covalently bonded molecules are quite close (within $\sim 10\%$) to the corresponding free atom values. This is particularly surprising for hydrogen, which has the most variable molecular environment. There is a general increase in "hardness" toward the upper right of the periodic table, as well as a gradient increase with increasing natural charge and decreasing radius. Clearly the standard ball-and-stick model of a molecule with uniform hard sphere atomic radii is inadequate, and more subtle features of the potential must be taken into account.

For the ionic radii, the periodic trends are less clear since there is a greater dependence on the identity of the counterion and degree of ionicity. This can be seen most dramatically for aluminum, where the natural charge on Al in Al_2O and AlN is similar, yet their longitudinal radii are at opposite ends of the general range of steric radii.

In view of these dependences, the free ion radii appear to be the "best" representative values, and these radii are compared with values calculated by previous methods in Table IV. Ionic natural steric radii of both cations and anions are generally larger than these previous values, because the former are independent of the attractive electrostatic forces, which brings ions closer than van der Waals contact, reducing the apparent radius. These results are consistent with Allinger's hypothesis.³

IV. ANISOTROPY OF ATOMIC VAN DER WAALS RADII

As a measure of steric anisotropy, one can determine an atomic “transverse radius” (r_{\perp}) perpendicular to the longitudinal radius. For example, one can calculate r_{\perp} for hydrogen in methane in a direction syn (s) to an adjacent C–H bond (1.980 Å) or in a direction anti (a) (1.693 Å) to that bond and “between” the other two C–H bonds. These radii are indicated in Fig. 5(a), which shows the “steric van der Waals surface” around one hydrogen atom in methane in one H–C–H plane. A helium atom was moved toward the hydrogen atom at 15° angle increments ranging from 90°–270° relative to the carbon to determine the contact distance (squares) and r_{\perp} (circles) at each angle. The effect of the adjacent bonds is to extend the van der Waals envelope from 1.420 Å (if the van der Waals radius were spherically isotropic) to between 1.693 and 1.980 Å in the perpendicular directions. Figure 5(b) displays a cross section of the steric surface in the plane perpendicular to the C–H bond containing the hydrogen atom, showing the distinct anisotropy.

The longitudinal and a selection of transverse radii for the representative set of molecules in Table II are listed side by side in Table V, the direction indicated with a superscript. Comparison of the transverse radius with the longitudinal radius shows the anisotropy of the steric potential about an atom. Using only the exterior or out-of-plane perpendicular transverse radii, the average anisotropy (measured by $r_{\perp} - r_l$) for several elements is listed in Table VI. These values are compared with the elliptical van der Waals radii calculated by Nyburg and Faerman,¹² who correlated the distances of closest approach of like atoms in crystals with angle, assumed the radius to be half the contact distance, and fit an ellipse (major and minor axes a and b) to these radii. They found no anisotropy for N and O, but significant anisotropy in the other elements. Steric radii also show lower average anisotropy for N and O and higher anisotropy for H, F, and Cl, but the results for sulfur disagree. The results in Tables V

TABLE IV. Comparison of the ionic radii in Table I with those estimated by previous methods.

Ion	$r_{\text{steric}}^{\text{NBO}}$	Previous values
H [−]	1.66	2.08, ^b 1.38 ^e
Li ⁺	0.87	0.78, ^a 0.60, ^b 0.94, ^c 0.74, ^e 0.71 ^f
Be ²⁺	0.75	0.34, ^a 0.31, ^b 0.27 ^f
N ^{3−}	1.90	1.71, ^b 1.46 ^f
O ^{2−}	1.62	1.32, ^a 1.40, ^b 2.40, ^d 1.31, ^e 1.35 ^f
F [−]	1.38	1.33, ^a 1.36, ^b 1.16, ^c 1.90, ^d 1.35, ^e 1.24 ^f
Na ⁺	1.13	0.98, ^a 0.95, ^b 1.17, ^c 1.35, ^d 1.11, ^e 0.97 ^f
Mg ²⁺	1.00	0.78, ^a 0.65, ^b 1.18, ^d 0.99, ^e 0.70 ^f
P ^{3−}	2.72	2.12 ^b
S ^{2−}	2.39	1.81, ^a 1.84, ^b 2.73, ^d 1.58 ^e
Cl [−]	2.06	1.81, ^a 1.81, ^b 1.64, ^c 2.25, ^d 1.71, ^e 1.80 ^f

^aReference 19.

^bReference 1, pp. 514.

^cReference 20.

^dReference 30.

^eReference 21.

^fReference 23.

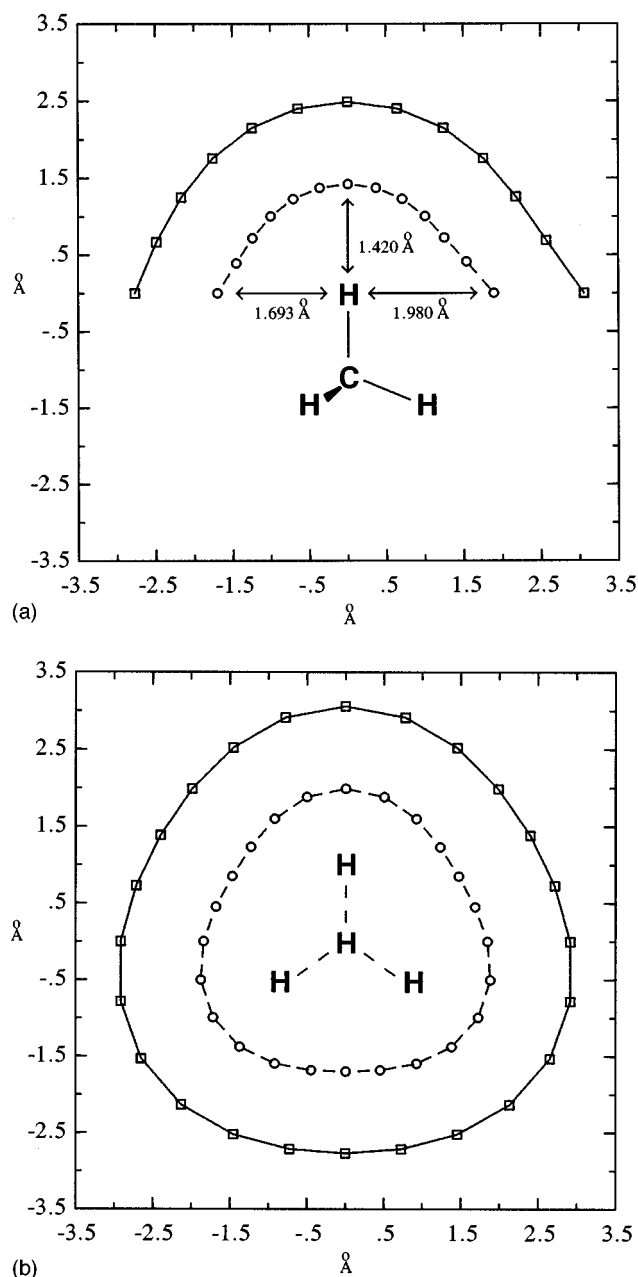


FIG. 5. (a) Steric van der Waals surface around one hydrogen atom in methane in the plane of another C–H bond. For angles relative to the carbon ranging from 90° to 270° in 15° increments, the position of the helium center of mass at which the $\Delta E_{\text{steric}}^{\text{NBO}} = kT$ for the CH₄–He is indicated by a square. The hydrogen radius (after subtraction of r_{He}) in that direction is indicated by a circle. (b) Cross section of the steric surface around a hydrogen atom in the plane perpendicular to the C–H bond and containing that hydrogen. The carbon (not shown) is directly below the center hydrogen. Symbols as in (a).

and VI show that the atomic transverse radius is greater than the longitudinal radius in both free molecules and molecular crystals.

The “insertion radius” (r_{ins}) is defined as the radius measured by inserting the probe atom toward a “crevice,” either (c) perpendicularly toward the center of a C–C bond between C–H bonds or (r) toward a methyl (CH₃) rotor,

TABLE V. Comparison of the longitudinal radii with selected transverse and insertion van der Waals radii for relevant molecules from Table II. r_{\perp} = transverse radius (perpendicular to bond); r_{ins} = insertion radius (into a crevice-like arrangement of atoms). Different approaches of the helium probe atom are indicated by superscripts.

Atom	Molecule	r_l	r_{\perp}	r_{ins}
H	LiH	1.645	2.213	
	BH ₃	1.461	1.439, ^c 1.914 ^a	
	C ₂ H ₆	1.426	1.718, ^a 3.038 ^b	
	CH ₄	1.420	1.693, ^d 1.980 ^c	
	C ₂ H ₄	1.415	1.774, ^c 1.864, ^a 3.136 ^b	
	C ₂ H ₂	1.396	1.701	
	H ₂	1.394	1.455	
	H ₂ CO	1.374	1.734, ^c 3.057 ^a	
	HCN	1.372	1.712	
	H ₂ S	1.362	1.717 ^a	
	CH ₃ SH	1.360	1.782 ^a	
	H ₂ CS	1.338	1.788, ^c 3.057 ^a	
	NH ₃	1.329	1.661, ^a 1.594 ^b	
	HNC	1.321	1.727	
	HCl	1.287	1.755	
	CH ₃ OH	1.247	1.466 ^a	
	HNO	1.222	1.497 ^a	
	H ₂ O	1.200	1.459, ^c 1.453 ^a	
	HF	1.103	1.278	
Li	Li ₂	2.700	2.983	
	LiH	2.128	2.358	
	LiF	1.394	1.350	
Be	BeO	0.921	0.739	
B	B ₂ O	2.255	1.979 ^c	
	B ₂ e ₃		1.901 ^a	
	BH ₃		1.428 ^c	
	BF ₃		2.039 ^c	
C	HNC	1.924	1.806	
	CO	1.885	1.627	
	H ₂ CS		2.250 ^c	
	CS ₂		2.095	
	H ₂ CO		1.933 ^c	
	C ₂ H ₂		1.931	
	HCN		1.887	
	CO ₂		1.764	
	C ₂ H ₄		1.990 ^c	1.984, ^g 2.212 ^f
	C ₂ F ₄		1.938 ^c	2.015, ^g 2.286 ^f
	CF ₄			1.932 ^g
	C ₂ H ₆			1.922, ^g 2.203 ^f
	CH ₄			1.897 ^g
N	HNO	1.756	1.655 ^c	
	HCN	1.739	1.823	
	NP	1.728	2.029	
	AlN	1.718	2.269	
	N ₂	1.678	1.669	
	NO	1.529	1.570	
	HNC		1.817	
	NH ₃	1.834		1.776 ^g
	NF ₃	1.748		1.807 ^g
O	MgO	1.738	1.787	
	H ₂ O	1.583	1.608 ^c	
	CH ₃ OH	1.582	1.722 ^c	
	BeO	1.578	1.551	
	H ₂ CO	1.532	1.531 ^c	
	CO	1.514	1.627	
	OS	1.507	1.830	
	CO ₂	1.506	1.687	
	HNO	1.493	1.548 ^a	
	NO	1.478	1.556	
	OF ₂	1.467	1.510 ^c	

TABLE V. (Continued.)

Atom	Molecule	r_l	r_{\perp}	r_{ins}
H	LiH			
	O ₂	1.438	1.497	
	B ₂ O		1.789	
	Al ₂ O		2.139	
F	LiF	1.431	1.350	
	PF ₃	1.357	1.420	
	BF ₃	1.354	1.759, ^c 1.861 ^a	
	C ₂ F ₄	1.343	1.513, ^c 1.583, ^a 2.471 ^b	
	CF ₄	1.334	1.645 ^d	
	HF	1.326	1.383	
	NF ₃	1.314	1.433 ^a	
	OF ₂	1.298	1.347 ^a	
	F ₂	1.273	1.335	
Na	Na ₂	3.156	3.413	
	NaCl	1.674	1.652	
Mg	MgO	2.225	2.002	
Al	Al ₂ O	2.914	2.446	
	AlN	1.049	2.495	
	Al ₂ O ₃		2.669	
P	P ₂	2.379	2.450	
	NP	2.340	2.279	
S	CH ₃ SH	2.226	2.341 ^c	
	S ₈	2.222	3.340 ^f	
	H ₂ S	2.190	2.311 ^c	
	CS ₂	2.139	2.141	
	H ₂ CS	2.133	2.190 ^c	
	S ₂	2.068	2.232	
Cl	OS	2.046	2.148	
	NaCl	2.046	1.926	
	HCl	1.905	2.032	
	CCl ₄	1.871	2.050 ^c	
	Cl ₂	1.857	2.013	

^a r_{\perp} measured facing the exterior of the molecule.

^b r_{\perp} measured facing the interior of the molecule.

^c r_{\perp} measured perpendicular to a planar or linear molecule.

^d r_{\perp} measured in a direction coplanar and anti to an adjacent C–H bond.

^e r_{\perp} measured in a direction coplanar and syn to an adjacent C–H bond.

^f r_{ins} measured perpendicular toward the center of a C–C bond between C–H bonds (crevice).

^g r_{ins} measured toward a methyl (CH₃) rotor, amine (NH₃), or planar CH₂ group, equidistant from the two or three hydrogens involved.

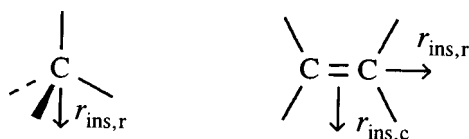
TABLE VI. Average anisotropy of several atomic radii calculated from steric analysis (measured as $r_{\perp} - r_l$) compared with the anisotropy estimated by Nyburg and Faerman (Ref. 12) (measured as the difference in elliptical axes, $a - b$).

Atom	$r_{\perp} - r_l$	b	a	$a - b$
H	0.31	1.01	1.26	0.25(sp^3)
N	0.06	1.60	1.32	0.38(sp^2)
O	0.09	1.54	1.54	0.00
F	0.16	1.30	1.38	0.08
S	0.09	1.60	2.03	0.43
Cl	0.15	1.58	1.78	0.20

TABLE VII. Calculated steric van der Waals radii (in angstroms) of helium, neon, and hydrogen in methane (approach along one C–H bond) at several different basis sets. [$r_{\text{H}} = R_{\text{vdw}}(\text{H}_3\text{CH}\cdots\text{He}) - r_{\text{He}}$].

Basis set	r_{He}	r_{Ne}	$R_{\text{vdw}}(\text{H}\cdots\text{He})$	r_{H}
STO-3G	1.034	1.064	2.330	1.296
3-21G	1.032	1.136	2.465	1.433
6-31G	1.069	1.211	2.492	1.423
6-31G*	1.069	1.211	2.493	1.424
6-31+G*	1.070	1.211	2.494	1.424
6-31G**	1.070	1.211	2.488	1.418
6-31++G**	1.070	1.211	2.491	1.421
6-311G**	1.089	1.236	2.493	1.404

amine (NH_3), or planar methylene (CH_2) group, equidistant from the two or three hydrogens involved, the radius extending in the directions below:



The rotor insertion radius $r_{\text{ins},r}$ added to the probe atom radius is effectively the minimum distance a probe atom can approach the central atom in a tetrahedral group. Based on $\text{CH}_3\cdots\text{CH}_3$, $\text{CH}_2\cdots\text{CH}_2$, and $\text{CH}_2\cdots\text{X}$ distances in several crystal hydrocarbons, Pauling assigned a value of 1.29 Å to a hydrogen radius in a methyl group and 2.0 Å to a methyl or CH_2 group as a whole. The radius of the methyl group, measured from the carbon center, varies with direction between the rotor insertion radius and the sum of the C–H bond length and the H radius. These ranges are 1.897–2.504 Å for CH_4 , 1.922–2.512 Å for ethane, and 1.984–2.491 Å for ethylene. Averaging this distance over all angles in a hemisphere yields values slightly greater than Pauling's estimate.

The effective surface encountered by a rare-gas atom in an elastic collision often extends well outside the midpoint between two atoms $\text{X}\cdots\text{Y}$ in XMY . For example, the rotor (CH_3) insertion radius for carbon in C_2H_6 is 1.922 Å. Charton¹⁶ calculated this carbon radius to be 1.72 Å, considerably lower. Use of Charton's empirical radii would predict greater penetration of another atom or group into the methyl rotor cavity than the steric repulsion would allow. Defining radii by partitioning the volume occupied by a functional group into spheroidal regions about the atoms does not reflect the true "surface" of the functional group, whereas defining a van der Waals radius or surface by directly probing the steric exchange repulsion takes account of the true shape of the electron distribution because no geometrical assumptions are made.

V. DEPENDENCE OF STERIC VAN DER WAALS RADII ON BASIS SET AND PROBE ATOM

A. Basis set dependence

The high transferability and basis set independence of NBOs³⁷ suggests that the calculated steric radii should be reasonably stable with respect to changes of basis. Calculated

TABLE VIII. Additive estimate R_{add} , actual steric van der Waals contact distance R_{vdw} using $\Delta E_{\text{steric}}^{\text{NBO}}(R_{\text{vdw}}) = kT$, and additivity difference ΔR_{add} (in Å) for selected interactions of molecules from Table II. Also given are the corrected estimates $R_{\text{cor}} = R_{\text{add}} - \kappa$ with remaining error ΔR_{cor} .

Contact	R_{add}	R_{vdw}	ΔR_{add}	R_{cor}	ΔR_{cor}
H–H \cdots H–H	2.788	2.392	+0.396	2.388	–0.004
H ₂ CO \cdots H–H	2.926	2.814	+0.112	2.826	+0.012
F–F \cdots H–H	2.667	2.575	+0.092	2.567	–0.008
H ₃ C–H \cdots H–CH ₃	2.840	2.532	+0.308	2.540	+0.008
H ₅ C ₂ –H \cdots H–C ₂ H ₅	2.852	2.589	+0.263	2.552	–0.037
H ₇ C ₃ –H \cdots H–C ₃ H ₇	2.858	2.598	+0.260	2.558	–0.040
CH ₃ O–H \cdots H–CH ₃	2.667	2.252	+0.285	2.367	–0.012
H ₂ N–H \cdots H–NH ₂	2.658	2.374	+0.284	2.358	–0.016
HO–H \cdots H–OH	2.400	2.307	+0.093	2.100	–0.207
F–H \cdots H–CH ₃	2.528	2.603	–0.075	2.428	–0.175
F–H \cdots H–F	2.206	4.046	–1.840	1.906	–2.140
H ₂ CO \cdots H–CH ₃	2.957	2.776	+0.181	2.857	+0.081
F–F \cdots H–CH ₃	2.698	2.584	+0.114	2.598	+0.014
N–N \cdots N–N	3.356	3.300	+0.056	3.356	+0.056
OCO \cdots OCO	3.012	3.017	–0.005	3.017	–0.005
F–F \cdots F–F	2.546	2.492	+0.054	2.492	+0.054
H–F \cdots F–F	2.599	2.565	+0.034	2.565	+0.034
Cl–Cl \cdots Cl–Cl	3.714	3.797	–0.083	3.797	–0.083
H–F \cdots F–H	2.652	3.818	–1.166	3.818	–1.166
H ₂ CO \cdots N–N	3.210	3.148	–0.062	3.148	–0.062
H ₂ CO \cdots F–F	2.805	2.805	0.000	2.805	0.000
H ₂ CO \cdots Cl–Cl	3.389	3.379	+0.010	3.379	+0.010
H ₂ CO \cdots OCH ₂	3.064	4.450	–1.386	4.450	–1.386

lated van der Waals radii for helium, neon, and hydrogen in methane (as measured from an approach of He along the C–H bond) are tabulated in Table VII for several different basis sets. The variations in the steric radius are seen to be quite small, at most a few hundredths of an angstrom. We calculated longitudinal and transverse radii for several molecules using the basis sets listed in Table VII and found similar consistency. For consistency, we have chosen the 6-31G* basis set for all recommended values, since this is the largest basis set available for third row atoms in GAUSSIAN 92.

B. Calibration of intermolecular steric radii for probe dependence

The van der Waals radii in Tables I, II, and V give accurate representations of the steric van der Waals surface for interaction with helium atoms. While these radii can be used directly for comparison with rare-gas atom scattering experiments, one is usually more interested in van der Waals radii of atoms in crystals or in solution. Paper I showed that the van der Waals radii for some molecules deviate markedly from additivity. However, comparison of additive and actual van der Waals contact distances in a variety of combinations of covalent molecules with small intermolecular delocalizations reveals a pattern to these deviations due to the distinct difference between a heavy atom, which has distinct core and valence shells, and hydrogen, which has only one 1s orbital. Deviations from additivity for a subset of these results are listed in Table VIII. We define the parameter κ as an additive constant depending only on the combination of hydrogens

and heavy atoms in direct contact and bonded to the contact atoms, such that the corrected distance $R_{\text{cor}} = R_{\text{add}} - \kappa$. For most examples of steric contacts between molecules in Table II, the following rough calibration should be applied to the additive estimates:

$$\begin{aligned} -\text{X}-\text{X}\cdots\text{X}- & \quad \kappa=0.0, \\ -\text{X}-\text{X}\cdots\text{H}- & \quad \kappa=0.1, \\ -\text{X}-\text{H}\cdots\text{H}- & \quad \kappa=0.3. \end{aligned} \quad (7)$$

This calibration brings about 90% of the contacts studied into agreement within $\pm 0.1 \text{ \AA}$ of the actual distance, the accuracy to which empirical estimates of van der Waals radii are usually given.^{2,38} Corrections to an effective radius would be $\kappa/2$ for like contacts and some fraction of κ for unlike contacts. Contributions from atoms further away tend to approximately cancel out, shown by the series methane, ethane, and propane. This calibration should not be applied to ions and ionic salts, since their radii show a strong dependence on the forms of the orbitals in contact.

C. Deviation from additivity due to inflexibility effects

While most molecules can be treated by the rough calibration above, the examples of $\text{F}-\text{H}\cdots\text{H}-\text{CH}_3$, $\text{F}-\text{H}\cdots\text{H}-\text{F}$, $\text{H}-\text{F}\cdots\text{F}-\text{H}$, $\text{HO}-\text{H}\cdots\text{H}-\text{OH}$, and formaldehyde dimer $(\text{H}_2\text{CO})_2$ ($\perp\text{HCH}$ planes) show that this does not hold for all cases. Formaldehyde dimer reaches van der Waals contact over 1.0 \AA outside that predicted by additivity, yet CO_2 dimer (which also has $-\text{C}=\text{O}$ in contact) shows near additivity. This difference is also true of the full self-consistent field (SCF) potential, which is significantly more repulsive for $\text{H}_2\text{CO}\cdots\text{OCH}_2$ than for $\text{OCO}\cdots\text{OCO}$. In H_2CO , the oxygen core and lone pairs show the largest increase in energy, while it is more evenly distributed among the σ_{CO} bonds and all three core orbitals in CO_2 . In contrast to methanol, methane, and ammonia, for example, like-atom contact in HF (and to a lesser extent H_2O) occurs far outside that predicted by additivity. Because most of the density is polarized toward one atom in a relatively inflexible system, orbitals in direct contact (here the HF or OH bonds) “absorb” an uncharacteristically large amount of the steric energy rather than the heavy atom core orbitals, increasing the contact distance. Larger molecules do not show this deviation.

Williams and Craycroft³⁹ attempted to separate the repulsive exchange and Coulombic interaction contributions to the overall potential (HF/6-31G** level) in CH_4 , NH_3 , and H_2O dimers using Morakuma analysis,⁴⁰ defining a hydrogen “van der Waals diameter” as the $\text{H}\cdots\text{H}$ distance at which the repulsive force reached 10^{-10} N . Their values for methane (2.548 \AA), ammonia (2.349 \AA), and water (2.181 \AA) decreased with an increasing charge on hydrogen (+0.186, +0.309, and +0.366, respectively), consistent with our results. However, the sum of the exchange and Coulombic interaction terms (+0.805 kcal/mol) accounted for only 39.8% of the total SCF energy (+2.024 kcal/mol). In contrast, steric analysis of H_2O dimer using the same geometry, distance, and basis set yields a steric energy of 1.399 kcal/

mol, accounting for 69.1% of the total SCF energy. The unexpectedly repulsive nature of the SCF potential at greater contact distances is better accounted for by the NBO steric exchange energy than the Morakuma exchange energy (only 0.224 kcal/mol in this case), and the larger steric contact distances in Table VIII better reflect the actual exchange repulsion.

The steric van der Waals contact distances reflect real steric effects between molecules, which can sometimes lead to unexpected deviations from behavior expected based on sums of empirical radii. The exceptions above caution against making the assumption of universal additivity (even with a constant correction) for van der Waals contacts, and help to explain the wide range of empirical estimates of van der Waals radii derived from contact distances that have been proposed since Pauling’s work.

VI. CONCLUSION

We have presented a new method for calculating steric van der Waals radii of free atoms and ions as well as atoms in molecules based on the difference in the NBO exchange repulsion energy between two or more species in van der Waals contact compared to the isolated species. In most cases intermolecular van der Waals contact distances calculated as sums of radii using a helium probe can be simply calibrated to come into approximate agreement with steric radii calculated for van der Waals complexes. The helium probe radii and the gradient of the steric exchange energy at van der Waals contact obey expected periodic trends and correlate with observed properties of van der Waals radii in molecular crystals and solution. Radii of atoms in covalent molecules can be correlated with the natural charge on the atom, tempered by effects from the molecular environment. Radii of atoms in ionic salts are more dependent on the electronegativity of the other atom(s) and are more sensitive to the shape of the electron distribution. Atomic radii are anisotropic, greater in the transverse than the longitudinal direction. How far the transverse radius “extends the envelope” is strongly dependent on the molecular environment.

The steric van der Waals radii were shown to be a consistent measure of the steric radius of an atom or molecule in any direction, independent of fits to specific experimental data, empirical potential parameters, or dispersion or other attractive terms in the interaction potential. Unlike previous empirical methods, the natural steric radius can be directly related to the temperature of the system, since one merely varies the value of the steric repulsion energy at which one defines “van der Waals contact” in Eq. (5) to obtain the temperature dependence of the van der Waals radius.

¹ L. Pauling, *The Nature of the Chemical Bond*, 3rd ed. (Cornell University Press, Ithaca, 1960), p. 260.

² S. S. Batsanov, *Russ. J. Inorg. Chem.* **36**, 1694 (1991).

³ N. A. Allinger, *Adv. Phys. Org. Chem.* **13**, 13 (1976).

⁴ N. A. Allinger, Y. H. Yuh, and J.-H. Lii, *J. Am. Chem. Soc.* **111**, 8551 (1989); J.-H. Lii and N. A. Allinger, *ibid.* **111**, 8576 (1989); N. A. Allinger, F. B. Li, and L. Q. Yan, *J. Comput. Chem.* **11**, 848.

⁵ P. K. Weiner and P. A. Kollman, *J. Comput. Chem.* **2**, 287 (1981); S. J.

- Weiner, P. A. Kollman, D. A. Case, U. C. Singh, C. Ghio, G. Alagona, S. Profeta, Jr., and P. Weiner, *J. Am. Chem. Soc.* **106**, 765 (1984); S. J. Weiner, P. A. Kollman, D. T. Nguyen, and D. A. Case, *J. Comput. Chem.* **7**, 230 (1986).
- ⁶B. R. Brooks, R. E. Bruccoleri, B. D. Olafson, D. J. States, S. Swaminathan, and M. Karplus, *J. Comput. Chem.* **4**, 187 (1983).
- ⁷M. Orozco and F. J. Luque, *J. Comput. Chem.* **14**, 587 (1982).
- ⁸A. K. Rappé, C. J. Casewit, K. S. Colwell, W. A. Goddard III, and W. M. Skiff, *J. Am. Chem. Soc.* **114**, 10024 (1992).
- ⁹A. Bondi, *J. Phys. Chem.* **68**, 441 (1964).
- ¹⁰Y. V. Zefirov and M. A. Porai-Koshits, *J. Struct. Chem.* **21**, 526 (1980); **27**, 239 (1986).
- ¹¹T. N. G. Row and R. Parthasarathy, *J. Am. Chem. Soc.* **103**, 477 (1981).
- ¹²S. C. Nyburg and C. H. Faerman, *Acta Crystallogr. Sect. B* **41**, 274 (1985); **43**, 106 (1987).
- ¹³L. S. Bartell, *J. Chem. Phys.* **32**, 827 (1960).
- ¹⁴C. Glidewell, *Inorg. Chim. Acta* **12**, 219 (1975); **20**, 113 (1976).
- ¹⁵M. Charton, *J. Am. Chem. Soc.* **101**, 7356 (1979).
- ¹⁶M. Charton, *J. Am. Chem. Soc.* **91**, 615 (1969).
- ¹⁷*Steric Effects in Drug Design*, edited by M. Charton and I. Motoc (Springer-Verlag, Berlin, 1983), pp. 58–91.
- ¹⁸Reference 1, pp. 505–509.
- ¹⁹Reference 1, p. 518.
- ²⁰B. S. Gourary and F. J. Adrian, *Solid State Phys.* **10**, 127 (1960).
- ²¹R. Narayan, *Pramana* **13**, 559 (1979).
- ²²Reference 1, p. 538.
- ²³Y. Marcus, *J. Sol. Chem.* **12**, 271 (1983); Y. Marcus, *Chem. Rev.* **88**, 1475 (1988).
- ²⁴J. Shanker and H. B. Agrawal, *Can. J. Phys.* **58**, 950 (1980).
- ²⁵R. T. Sanderson, *Chemical Periodicity* (Van Nostrand Reinhold, New York, 1960), pp. 25–27.
- ²⁶Reference 1, p. 92.
- ²⁷L. H. Thomas, *J. Chem. Phys.* **22**, 1758 (1954).
- ²⁸B. M. Deb, R. Singh, and N. Sukumar, *J. Mol. Struct. (Theochem)* **259**, 121 (1992).
- ²⁹See for example, K. D. Sen and P. Politzer, *J. Chem. Phys.* **90**, 4370 (1989); R. R. Contreras and A. J. Smith, *J. Mol. Struct. (Theochem)* **282**, 143 (1993).
- ³⁰R. H. Stokes, *J. Am. Chem. Soc.* **86**, 979 (1964).
- ³¹S. Miertus, J. Bartos, and M. Trebaticka, *J. Mol. Liq.* **33**, 139 (1987).
- ³²H. Iijima, J. B. Dunbar Jr., and G. R. Marshall, *Proteins: Structure, Function, and Genetics* **2**, 330 (1987).
- ³³I. Motoc and G. R. Marshall, *Chem. Phys. Lett.* **116**, 415 (1985).
- ³⁴J. K. Badenhoop and F. Weinhold, *J. Chem. Phys.* **107**, 5406 (1997), preceding paper.
- ³⁵J. P. Foster and F. Weinhold, *J. Am. Chem. Soc.* **102**, 7211 (1980); A. E. Reed and F. Weinhold, *J. Chem. Phys.* **78**, 4066 (1983); A. E. Reed, R. B. Weinstock, and F. Weinhold, *J. Chem. Phys.* **83**, 735 (1985); A. E. Reed and F. Weinhold, *J. Chem. Phys.* **83**, 1736 (1985).
- ³⁶M. J. Frisch, G. W. Trucks, M. Head-Gordon, P. M. W. Gill, M. W. Wong, J. B. Foresman, B. G. Johnson, H. B. Schlegel, M. A. Robb, E. S. Repogle, R. Gomperts, J. L. Andres, K. Raghavachari, J. S. Binkley, C. Gonzalez, R. L. Martin, D. J. Fox, D. J. Defrees, J. Baker, J. J. P. Stewart, and J. A. Pople, GAUSSIAN 92, Revision A, Gaussian, Inc., Pittsburgh, PA, 1992.
- ³⁷J. E. Carpenter and F. Weinhold, *J. Am. Chem. Soc.* **110**, 368 (1988).
- ³⁸Reference 1, pp. 259–264.
- ³⁹D. E. Williams and D. J. Craycroft, *J. Phys. Chem.* **91**, 6365 (1987).
- ⁴⁰K. Morakuma, *J. Chem. Phys.* **55**, 1236 (1971).
- ⁴¹Y. V. Zefirov and P. M. Zorkii, *J. Struct. Chem.* **15**, 102 (1974); **17**, 644 (1976).